Article

Improving the flexibility of genetically encoded voltage indicators via intermolecular FRET

Lee Min Leong,[1,2] Bok Eum Kang,[1] and Bradley J. Baker[1,2,*]

[1]Brain Science Institute, Korea Institute of Science and Technology, Seongbuk-gu, Seoul, Republic of Korea and [2]Division of Bio-Medical Science and Technology, KIST School, Korea University of Science and Technology (UST), Seoul, Republic of Korea

ABSTRACT   A new family of genetically encoded voltage indicators (GEVIs) has been developed based on intermolecular Förster resonance energy transfer (FRET). To test the hypothesis that the GEVI ArcLight functions via interactions between the fluorescent protein (FP) domains of neighboring probes, the FP of ArcLight was replaced with either a FRET donor or acceptor FP. We discovered relatively large FRET signals only when cells were cotransfected with both the FRET donor and acceptor GEVIs. Using a cyan fluorescent protein donor and an RFP acceptor, we were able to observe a voltage-dependent signal with an emission peak separated by over 200 nm from the excitation wavelength. The intermolecular FRET strategy also works for rhodopsin-based probes, potentially improving their flexibility as well. Separating the FRET pair into two distinct proteins has important advantages over intramolecular FRET constructs. The signals are larger because the voltage-induced conformational change moves two FPs independently. The expression of the FRET donor and acceptor can also be restricted independently, enabling greater cell type specificity as well as refined subcellular voltage reporting.

SIGNIFICANCE   Intermolecular Förster resonance energy transfer (FRET) genetically encoded voltage indicators demonstrate that the FP domain of neighboring probes get closer and/or orient better upon depolarization of the plasma membrane. This interaction enables any fluorescent FRET pair to be utilized to monitor changes in membrane potential and can restrict expression to only cells expressing both the FRET donor and acceptor versions of the genetically encoded voltage indicators.

INTRODUCTION

The ability of genetically encoded voltage indicators (GEVIs) to optically report changes in membrane potential offers the promise of monitoring neuronal activities from multiple cell populations in neuronal circuits simultaneously. Despite the impressive progress in the development of GEVIs (1–7), this multiple observation potential remains largely theoretical. A recent, independent comparison of GEVIs revealed that, whereas most perform well in cultured, single-cell recordings, the only consistent signal observed in vivo was from ArcLight (8). ArcLight's brightness, dynamic range, and voltage sensitivity make it one of the easiest GEVIs to use. However, the need to average trials indicates that ArcLight's signal also needs improvement.

To enhance the optical signal of ArcLight, we have sought to elucidate the mechanism mediating the voltage-

dependent fluorescence change upon plasma membrane potential fluctuations. ArcLight consists of a pH-sensitive fluorescent protein (FP), super ecliptic pHluorin A227D (SEpH) (9), fused to the voltage-sensing domain (VSD) of the *Ciona intestinalis* voltage-sensing phosphatase (10). The SEpH FP in ArcLight contains a unique mutation that introduces a negative charge to the exterior of the β-can structure. A previous report from our lab suggested that this external negative charge interacts with a neighboring FP because mutations to SEpH that favor the monomeric form of the FP diminished the voltage-dependent signal by at least 70% (11). Taking advantage of this FP dimerization architecture, we were able to develop the red-shifted GEVI, Ilmol, by replacing SEpH with the FP, dTomato (5).

Our initial goal was to test the ability of the FP domain of ArcLight-derived GEVIs to interact with neighboring probes. To test that hypothesis, we replaced SEpH in ArcLight with FPs having spectral properties capable of Förster resonance energy transfer (FRET). Fig. 1 provides a schematic overview of the GEVIs used in this report. Previous FRET versions of GEVIs have used intramolecular FRET,

---
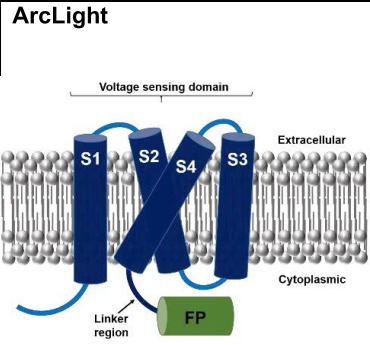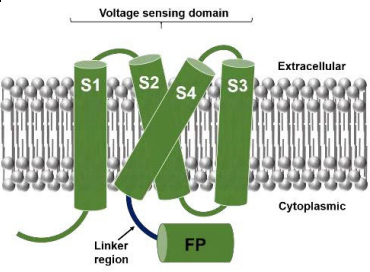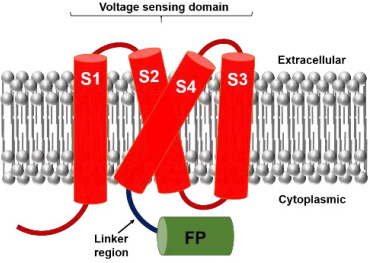
	Properties	GEVI Compsition
ArcLight 	ArcLight has a large optical signal but slow kinetics.	**VSD** **Linker** **FP** ArcLight-CFP: *Ciona* based VSD – YSHQQMKAGDP – Cerulean ArcLight-YFP: *Ciona* based VSD – YSHQQMKAGDP – Venus ArcLight-Clover: *Ciona* based VSD – YSHQQMKAGDP – Clover ArcLight-mRuby2: *Ciona* based VSD – YSHQQMKAGDP – mRuby2
Bongwoori-R3 	Bongwoori-R3 has a comparable optical signal to ArcLight with faster kinetics.	**VSD** **Linker** **FP** BongwooriR3-CFP: *Ciona* based VSD – YSRQQGDP – Cerulean BongwooriR3-YFP: *Ciona* based VSD – YSRQQGDP – Venus BongwooriR3-dTomato: *Ciona* based VSD – YSRQQGDP – dTomato
CC1 	CC1 requires a strong de-polarization in order to see the optical response.	**VSD** **Linker** **FP** CC1-CFP: *Ciona* based VSD – YSHQQMKASSRRTISQNKRRYR – Cerulean CC1-YFP: *Ciona* based VSD – YSHQQMKASSRRTISQNKRRYR – Venus

FIGURE 1 Description of the GEVIs used in this study. ArcLight (10), Bongwoori (6), and CC1 (12) exhibit different kinetics and respond to different voltages. Here, the GEVIs are represented as monomers, and subsequent figures will show potential dimer interactions. Because inter-FRET GEVIs can involve different combinations of cotransfection, the color coding of the VSD for each construct is maintained throughout this report.

in which the donor and acceptor chromophores are contained in the same protein (13–16). Here, the FRET pair is split between two distinct proteins by fusing the donor FP to one VSD while the acceptor is fused to a separate VSD, enabling intermolecular FRET (inter-FRET). Cotransfection of Arc-Light derivatives when SEpH was replaced by the cyan fluorescent protein (CFP), Cerulean, or the yellow fluorescent protein (YFP), Venus, resulted in robust inter-FRET signals. These inter-FRET signals prove that the FP domains of Arc-Light are capable of interacting. Furthermore, inter-FRET GEVIs consisting of green/red FRET pairs also yielded robust signals, indicating that the entire visible spectrum is open for future probe development as well as the potential for far-red/infrared FRET pairs and may represent an improved configuration for imaging voltage.

This new family of inter-FRET GEVIs offers several potential advantages over previously reported probes. The ratiometric nature of the inter-FRET signal may enable the removal of motion artifacts due to blood flow and respiration during in vivo recordings. Inter-FRET GEVIs may also improve two-photon probe development because ArcLight-derived GEVIs are no longer restricted to using the pH-sensitive SEpH FP. Any bright two-photon FP can now be used as the donor in conjunction with an appropriate FRET

acceptor FP. Cell type specificity may also be improved because different promoters can be used to express the donor and acceptor inter-FRET partners. Only cell types that express both promoters will be capable of yielding voltage-dependent inter-FRET signals. As a proof of principal, we were also able to elicit a voltage-dependent optical signal from a rhodopsin-based GEVI via intermolecular FRET.

MATERIALS AND METHODS

Plasmid design and construction

ArcLight-Cerulean, ArcLight-Venus, ArcLight-Clover, ArcLight-mRuby2, Bongwoori-R3-Cerulean, Bongwoori-R3-Venus, Bongwoori-R3-dTomato, CC1-Cerulean, and CC1-Venus were constructed by replacing the SEpH FP in ArcLight with the respective FPs. The farnesylated versions of the FPs were synthesized (Integrated DNA Technologies, Coralville, IO). For the ArcLight and Bongwoori-R3 constructs, the FPs were designed to have a 5′ BamHI restriction site and a 3′ stop codon followed by an XhoI site. The FPs for the CC1 constructs were designed to have a 5′ BamHI restriction site and a 3′ stop codon followed by an XhoI site. The Ace2N construct was designed to have a 5′ NheI site and a 3′ stop codon followed by an XhoI site. Conventional one-step and two-step PCR overlap were used to generate monomeric versions of FPs and the Ace2N construct. Primers were designed to introduce the restriction sites and the monomeric mutations in the FPs. The backbone vector used in this study is pcDNA3.1 with a CMV promoter.

Cell culture and transfection

Human embryonic kidney (HEK) 293 cells were cultured in Dulbecco's Modified Eagle Medium (Gibco, USA) supplemented with 10% fetal bovine serum (Gibco) at 37°C, 100% humidity, and 5% CO_2. For transfection, HEK 293 cells were suspended using 0.25% trypsin-EDTA (Gibco), then plated onto poly-L-lysine (Sigma-Aldrich, St. Louis, MO)-coated #0 coverslips (0.08–0.13 mm thick and 10 mm diameter; Ted Pella, Redding, CA) at 70% confluency. Transient transfection was carried out with Lipofectamine 2000 (Invitrogen, Carlsbad, CA) according to the manufacturer's protocol. Equal concentrations of DNA were used for co- and tritransfection experiments.

Hippocampal neurons were cultured according to an approved animal experiment protocol by the Institutional Animal Care and Use Committee at KIST (animal protocol 2016-082), as described previously (6). In brief, the hippocampi of embryonic day 17 C57BL/6 mice (Koatech Laboratory Animals, Pyeongtaek, South Korea) were dissected and treated with 0.125% trypsin-EDTA solution (Gibco) for 15 min in a 37°C water bath. DNase I (Sigma-Aldrich) was added for 30 s after digestion. The cells were then rinsed with plating media composed of 10% fetal bovine serum and 1% penicillin-streptomycin (Gibco) in Dulbecco's Modified Eagle Medium and subjected to mechanical trituration. Dissociated neurons were then plated onto poly-D-lysine (Sigma-Aldrich)-coated #0 coverslips at 5×10^4 cells/mL density. The plating media was replaced with maintenance media composed of Neurobasal medium (Gibco) supplemented with 2% B27 supplement (Gibco) and 1% penicillin-streptomycin. 50% of maintenance media was exchanged every 3 days. Transient transfection of cultured mouse hippocampal neurons was done 5–7 days in vitro using Lipofectamine 2000 according to the manufacturer's protocol, and experiments were on days in vitro 8–12. Equal concentrations of DNA plasmids were used for cotransfection experiments.

Electrophysiology

Coverslips with transiently transfected cells were inserted into a patch chamber (Warner Instruments, Hamden, CT) with its bottom side covered with a #0 thickness coverglass for simultaneous voltage-clamp and fluorescence imaging. The chamber was kept at 34°C throughout the experiment and perfused with bath solution (150 mM NaCl, 4 mM KCl, 1 mM $MgCl_2$, 2 mM $CaCl_2$, 5 mM D-glucose and 5 mM HEPES (pH 7.4)). Filamented glass capillary tubes (1.5 mm/0.84 mm; World Precision Instruments, Sarasota, FL) were pulled by a micropipette puller (Sutter Instrument, Novato, CA) before each experiment to pipette resistances of 3–5 MΩ for HEK 293 cells and 3–6 MΩ for cultured primary neurons. The pipettes were filled with intracellular solution (120 mM K-aspartate, 4 mM NaCl, 4 mM $MgCl_2$, 1 mM $CaCl_2$, 10 mM EGTA, 3 mM Na_2ATP, and 5 mM HEPES (pH 7.2)) and held by a pipette holder (HEKA Elektronik, Germany) mounted on a micromanipulator (Scientifica, Uckfield, UK). Whole-cell voltage-clamp and current-clamp recordings of transfected cells were conducted using a patch-clamp amplifier (HEKA, Lambrecht, Germany). A holding potential of −70 mV was used for all recordings, including neuronal recordings with cultured neurons until a switch to current-clamp mode.

Fluorescence microscopy

An inverted microscope (IX71; Olympus, Japan) equipped with a 60× oil-immersion lens with 1.35 NA was used for epifluorescence imaging. A 470 nm light-emitting diode (LED) (bandwidth: 25 nm) placed in a 4-wavelength LED housing (LED4D242; Thorlabs, Newton, NJ) was used for the experiments of Ace2N with farnesylated Clover. A four-channel LED driver and its software (DC4100; Thorlabs) were used to control the LED. For the other experiments, the light source was a 75 W Xenon arc lamp (Osram, Munich, Germany) placed in a lamp housing (Cairn, UK). CFP was imaged using a filter cube consisting of an excitation filter (FF434/17), a dichroic mirror (FF452-Di01), and an emission filter (FF01-479/40). YFP was imaged with a filter cube consisting of an excitation filter (FF497/16), a dichroic mirror (FF516-Di01), and an emission filter (FF01-535/22). GFP was imaged using a filter cube consisting of an excitation filter (FF02-472/30), a dichroic mirror (FF495-Di03), and an emission filter (FF520/40). RFP was imaged with a filter cube consisting of an excitation filter (FF01-561/14), a dichroic mirror (Di02-R561), and an emission filter (FF01–609/54). CFP-YFP FRET was imaged using an optical splitter (Cairn, UK) consisting of two filter cubes. The first was composed of excitation filter (FF434/17) and a dichroic mirror (FF452-Di01) without emission filter, and the second cube resided in an optical splitter (Cairn, UK) consisting of an emission filter (FF497/16), a dichroic mirror (FF510-Di02), and emission filter (FF01-535/22). GFP-RFP FRET was imaged using two filter cubes. The first was composed of excitation filter (FF475/23) and a dichroic mirror (FF495-Di02) without emission filter, and the second cube in the optical splitter consisted of an emission filter (FF520/40), a dichroic mirror (FF560-Di01), and emission filter (FF01-645/75). CFP-RFP FRET was imaged in a similar manner. The first cube was composed of an excitation filter (FF434/17) and a dichroic mirror (FF452-Di01) without emission filter. The second cube consisted of an emission filter (FF497/16), a dichroic mirror (FF510-Di02), and emission filter (FF01-645/75 or FF585/29). GFP-RFP FRET was also imaged using two filter cubes. The first was composed of excitation filter (FF475/23) and a dichroic mirror (FF495-Di02) without emission filter, and the second cube consist of emission filter (FF520/40), a dichroic mirror (FF560-Di01), and emission filter (FF01-645/75) (all by Semrock, Rochester, NY). Two cameras were mounted on the microscope through a dual port camera adaptor (Olympus). A slow speed color charge-coupled-device camera (Hitachi, Tokyo, Japan) was used to aid in locating cells during patch-clamp experiments. Fluorescence changes of the voltage indicators were typically recorded at 1 kHz frame rate by a high-speed CCD camera (RedShirtImaging, Decatur, GA), unless otherwise specified. All the relevant optical devices were placed on a vibration isolation platform (Kinetic Systems, Boston, MA) to avoid any vibrational noise during patch-clamp fluorometry experiments.
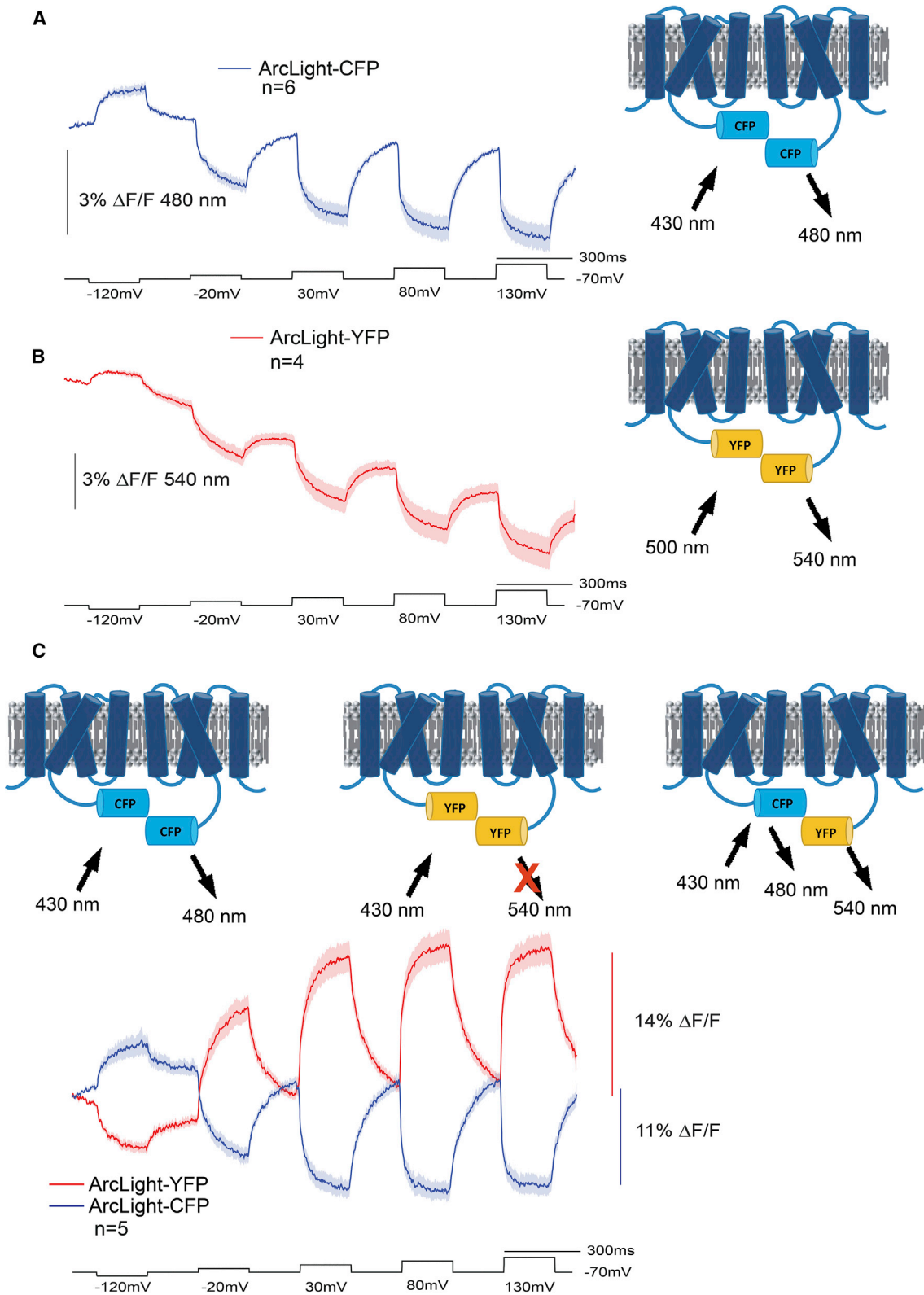
FIGURE 2 Intermolecular FRET GEVIs. (*A*) Optical traces from ArcLight-CFP. HEK 293 cells expressing only ArcLight-CFP were voltage clamped at a holding potential of −70 mV and subjected to a five-pulse protocol (*black trace*). Excitation light for ArcLight-CFP was 430 nm. The optical trace in blue was acquired at 1 kHz. The solid blue line represents the mean from six cells. The shaded area is the standard error (SE) of the mean. (*B*) Optical traces from ArcLight-YFP. HEK 293 cells expressing only ArcLight-YFP were voltage clamped as described in (*A*). Excitation light was 500 nm for ArcLight-YFP. The solid red line represents the mean from four cells. (*C*) Optical traces from intermolecular FRET GEVIs. The GEVI schematics represent the three potential

Data acquisition and analysis

Resulting images from patch-clamp fluorometry were acquired and analyzed for initial parameters, such as fluorescence change [$\Delta F = F_x - F_0$] or fractional fluorescence change values [$\Delta F/F = ((F_x - F_0)/F_0) \times 100$] by NeuroPlex software (RedShirtImaging) and Microsoft Excel (Microsoft, Redmond, WA). The acquired data from whole-cell voltage-clamp experiments of HEK 293 cells were averaged for eight trials, unless otherwise noted. The number of cells tested (*n*) are reported in each figure. Data were collected from recorded cells that did not lose their seals during the whole-cell voltage-clamp recording. $\Delta F/F$ values for the tested voltage pulses were plotted in OriginPro 2016 (OriginLab). A $\Delta F/F$ trace versus time graph for each cell was also fitted for either double- or single-exponential decay functions in OriginPro 2016 as described previously (12).

RESULTS

Cotransfection of inter-FRET GEVIs yields voltage-dependent optical signals

Introduction of monomer-inducing mutations to the FP of ArcLight-type GEVIs resulted in a substantial reduction of the voltage-dependent optical signal (11). That result suggested the possibility that dimerization of the FP domain was necessary for the optical response of ArcLight. To test that hypothesis, we employed inter-FRET imaging by replacing the SEpH FP in ArcLight with either the CFP Cerulean (17) or the YFP Venus (18). These two constructs are denoted as ArcLight-CFP or ArcLight-YFP, respectively. Fig. 2 compares the optical signals from HEK cells expressing either the FRET donor construct alone, Arc-Light-CFP (Fig. 2 *A*), the FRET acceptor construct alone, ArcLight-YFP (Fig. 2 *B*), or the coexpression of the FRET pair (Fig. 2 *C*). Whole-cell voltage clamp of HEK cells expressing only ArcLight-CFP yielded a small voltage-dependent signal that reached a maximum of ∼3% $\Delta F/F$ (comparison of the relative fluorescent changes for the GE-VIs in this report can be found in Table S1). The signal size from cells expressing only ArcLight-YFP was roughly the same but also exhibited a noticeable degree of bleaching. Cotransfection of ArcLight-CFP and ArcLight-YFP yielded a larger optical response, in which the ArcLight-YFP signal inverted its polarity as compared with recordings from cells expressing ArcLight-YFP only. This reciprocal change in fluorescence was indicative of a FRET signal. Upon depolarization of the plasma membrane, the FRET efficiency improved as the donor chromophore fluorescence was reduced by over 10% $\Delta F/F$/100 mV and the acceptor fluorescence was increased by 14% $\Delta F/F$/100 mV, indicating that the distance between the chromophores had decreased and/or that the orientation of the chromophores had improved during the depolarization of the plasma membrane.

Because no effort was made to optimize the interaction of the molecules containing the FRET FP pairs, the optical signal in Fig. 2 *C* is a mixture of ArcLight-CFP/ArcLight-YFP as well as the potential ArcLight-CFP/ArcLight-CFP and ArcLight-YFP/ArcLight-YFP associations (cross-contamination of the ArcLight-CFP GEVI signal in the YFP channel can be seen in Fig. S1). However, the ArcLight-CFP-only signal (Fig. 2 *A*) and the ArcLight-YFP-only signal (Fig. 2 *B*) are small. In addition, the wavelength of excitation in Fig. 2 *C* was 430 nm, which further reduces the ArcLight-YFP/ArcLight-YFP signal because the excitation peak for Venus is near 500 nm. No voltage-dependent signal was observed for HEK cells only expressing ArcLight-YFP when excited at 430 nm (Fig. S2). Despite this imperfect system, the inter-FRET GEVI signal exceeds the optical signals seen for other GEVIs that use intramolecular FRET, such as Nabi (13) or VSFP-Butterfly (16).

The voltage sensor domain determines the speed of the optical response

The Bongwoori family of GEVIs are ArcLight-derived sensors that have faster kinetics (6,12). To determine whether the interaction between Cerulean and Venus would alter the kinetics, the ArcLight VSD was replaced with the BongwooriR3 VSD. When the YFP/CFP inter-FRET versions of Bongwoori-R3 are expressed in HEK 293 cells, a robust signal is again seen with faster kinetics (Fig. 3, *A*–*C*; Table S3) demonstrating that the kinetics of the voltage-dependent optical signal is primarily determined by the VSD.
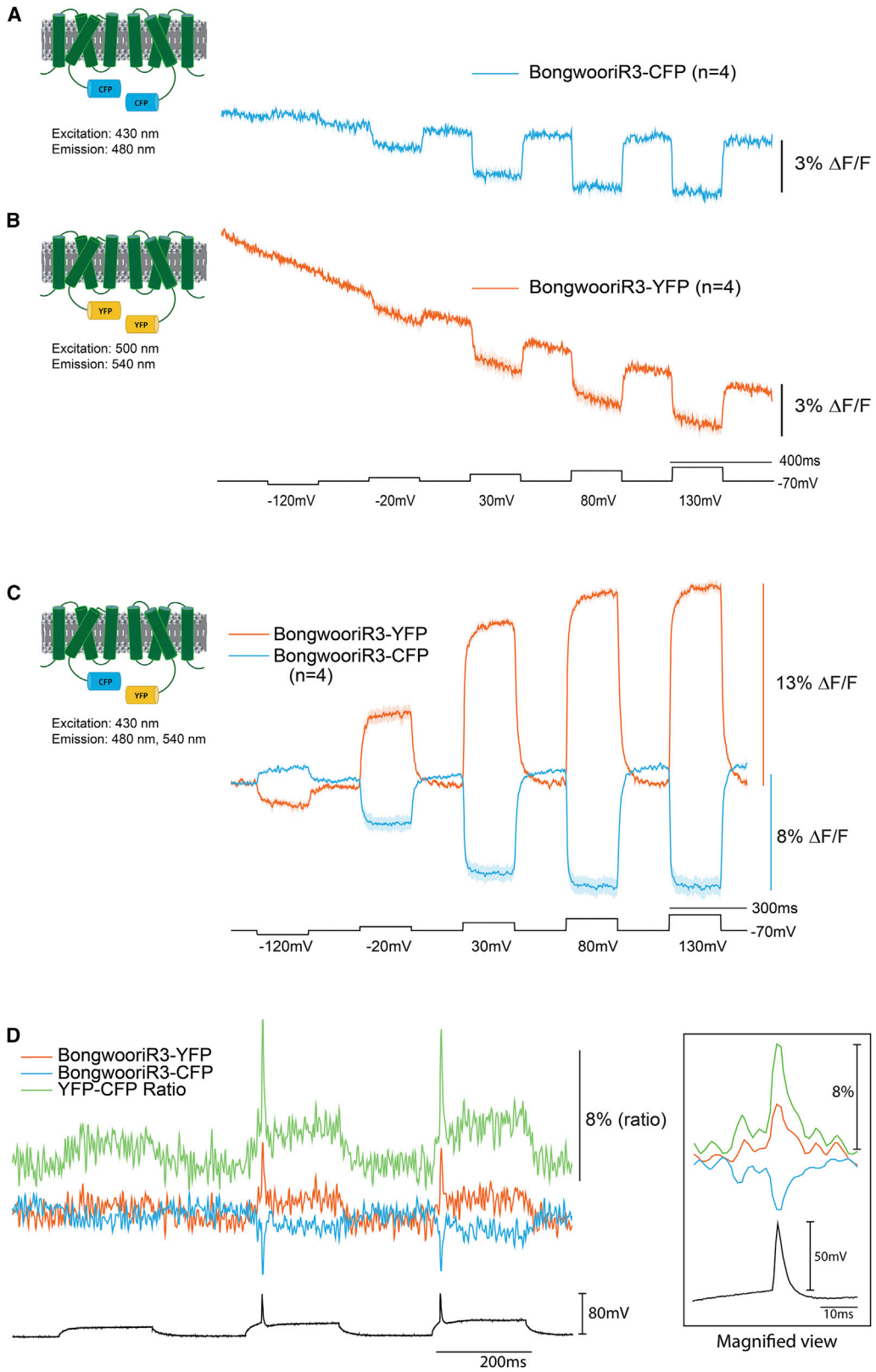
Because this version is faster, we also expressed this FRET pair in cultured hippocampal neurons, resulting in a fast, ratiometric signal during action potentials (Fig. 3 *D*).

Monomeric mutations to the FP do not abolish the voltage-dependent FRET signal

Most derivatives of GFP from *Agriocnemis victoria* exist as protein dimers. An exception is CFP because of the N146I mutation rotating the seventh β-strand and exposing the side chain of Y145 (numbering based on GFP amino acid sequence) that interferes with dimer formation (19). However, because CFP can form dimers in the mM range (20), the effective protein concentration at the plasma membrane may be sufficient for some dimerization because diffusion is limited to two-dimensional space. We therefore introduced monomeric favoring mutations to the FPs of the ArcLight inter-FRET pairs in an attempt to abolish the FRET signal.

The three mutations to GFP that favor the monomeric form are A206K, L221K, and F223R (21). The L221K mutation exhibited very little effect on the voltage-dependent FRET signal (Fig. 4). The YFP signal was virtually the same (14%

interactions upon cotransfection of HEK 293 cells with ArcLight-CFP and ArcLight-YFP. Excitation at 430 nm limits the contribution of the ArcLight-YFP/ArcLight-YFP interactions because the excitation peak of YFP is near 500 nm. Optical emissions at 480 and 540 nm were collected simultaneously with the use of an optical splitter (see Materials and methods). The blue trace is the 480 nm emission average from five cells voltage clamped as described in (*A*). The red trace is the 540 nm emission average.

A

BongwooriR3-CFP (n=4)

Excitation: 430 nm
Emission: 480 nm

3% ΔF/F

B

BongwooriR3-YFP (n=4)

Excitation: 500 nm
Emission: 540 nm

3% ΔF/F

400ms
-70mV

-120mV   -20mV   30mV   80mV   130mV

C

BongwooriR3-YFP
BongwooriR3-CFP
(n=4)

Excitation: 430 nm
Emission: 480 nm, 540 nm

13% ΔF/F

8% ΔF/F

300ms
-70mV

-120mV   -20mV   30mV   80mV   130mV

D

BongwooriR3-YFP
BongwooriR3-CFP
YFP-CFP Ratio

8% (ratio)

80mV

200ms

8%

50mV

10ms

Magnified view

(legend continued on next page)

compared with 13%), and the CFP signal was slightly diminished (8% compared with 11%). The A206K mutation, which is the most utilized monomeric mutation, slightly affected the YFP signal (10% compared with 14%) but nearly cut the CFP signal in half (6% compared with 11%). The F223R mutation had the largest effect, reducing the YFP signal from 14% to below 4% and the CFP signal from 11 to 2%.

This large variation in the effects on the voltage-dependent optical signal suggests there may be some dimerization of the FP domain at the plasma membrane. However, the monomeric mutations were unable to completely destroy the optical signal, suggesting that other FPs from different organisms with different wavelengths could also be used for inter-FRET GEVI development.

Expanding the spectrum of the inter-FRET GEVI signals

The ArcLight family of GEVIs utilizes the VSD from the gene family of voltage-sensing phosphatases. Recently, it has been shown that the voltage-sensing phosphatase can dimerize (22). Dimerization via the VSD of the phosphatase protein could explain why monomeric mutations to the FP domain failed to eliminate the voltage-dependent optical signal. Dimerization of the VSD would enable the use of any FRET pair for imaging voltage.

Replacement of the SEpH FP with the red-shifted FP mRuby2 (23) again yielded a GEVI with a modest voltage-dependent signal of under 3% ΔF/F/100 mV when expressed in HEK 293 cells (Fig. 5 A). To facilitate the FRET signal for the FP mRuby2, we also replaced SEpH in ArcLight with the GFP-derived FP Clover (23). HEK 293 cells expressing only ArcLight-Clover yielded an even smaller voltage-dependent signal below 2% ΔF/F/100 mV (Fig. 5 B). However, when ArcLight-Clover and ArcLight-mRuby2 were cotransfected into HEK 293 cells, a much improved voltage-dependent signal was observed (Fig. 5 C). The ArcLight-Clover signal decreased by 7% during a 100 mV depolarization step, whereas the ArcLight-mRuby2 signal increased by nearly 11%. Like the CFP/YFP version, depolarization of the plasma membrane increased the inter-FRET efficiency, indicating that the chromophores of the FPs were getting closer and/or moving into a better orientation for energy transfer.

Investigating the potential multimeric association of ArcLight-derived GEVIs enabled a voltage-dependent optical signal separated by 200 nm from the excitation wavelength

FRET signals for both the CFP/YFP and the GFP/RFP inter-FRET pairs indicated that the FP domain of ArcLight-derived GEVIs are in close proximity which suggested that the association was occurring at least in part via the VSD. To determine the extent of a possible multimerization, we attempted an inter-FRET measurement from CFP to RFP via YFP. Triple transfection of HEK 293 cells with the BongwooriR3 GEVI fused to CFP, YFP, and RFP resulted in a voltage-dependent signal that exhibited an optical signal over 160 nm away from the excitation wavelength (Fig. 5 D). Using a different filter set, a voltage-dependent signal over 225 nm away from the excitation wavelength was observed when HEK cells were transfected with ArcLight-Cerulean/ArcLight-Venus/ArcLight-mRuby2 (Fig. 5 E).

To determine whether the large optical signal was due to a contiguous FRET signal from CFP to YFP to RFP, we also imaged HEK cells expressing only the inter-FRET CFP/RFP Bongwoori-R3 constructs (Fig. 5 F). Excitation at 420 nm yielded a voltage-dependent optical signal at 585 nm without the presence of YFP. Despite the reduced overlap of Cerulean's emission profile to dTomato's excitation spectra when compared with Venus, the broad emission shoulder of Cerulean enabled FRET to dTomato. Comparison of the signals from HEK cells expressing the triple-FRET constructs (CFP/YFP/RFP) with HEK cells only expressing the CFP/RFP versions showed a similar dynamic range for RFP (20% ΔF/F/200 mV), but the CFP signal for the triple-transfected cells was twice that of cells not expressing the YFP version. This disparity could be the result of CFP directly transferring energy to RFP in both experiments. Because the presence of the VSD fused to YFP failed to alter the RFP signal, it is unlikely that trimers or tetramers of the VSD exist.

Monitoring the movement of a single FP using heterogeneous VSDs

The movement of S4 has been shown to mediate the voltage-dependent optical signal for ArcLight-derived GEVIs (11,24,25). One potential reason the inter-FRET signal is relatively larger than earlier FRET constructs (13,14,16,26) is that the voltage-induced conformational change is amplified. Because both the donor and acceptor FPs are moving independently, the net distance/orientation change may be greater. Previous FRET GEVIs incorporated both the donor and acceptor FPs in the same molecule, thereby limiting the change in distance/orientation.

To visualize the individual contribution of the FRET donor or FRET acceptor on the voltage signal, we utilized

---

FIGURE 3   The inter-FRET signal from BongwooriR3-derived GEVIs. Voltage-induced optical response of HEK cells expressing BongwooriR3-CFP (*A*) or Bongwoori-YFP (*B*). (*C*) Optical response from HEK cells coexpressing BongwooriR3-Cerulean and BongwooriR3-Venus. (*D*) The trace is from a hippocampal neuron in culture under whole-cell current clamp coexpressing BongwooriR3-Cerulean and BongwooriR3-Venus. The black trace is voltage. The blue trace is CFP emission at 480 nm. The red trace is from YFP emission at 540 nm. Excitation wavelength is 430 nm. The green trace is the ratio of YFP/CFP fluorescence. Inset is a time expanded view of the first action potential.
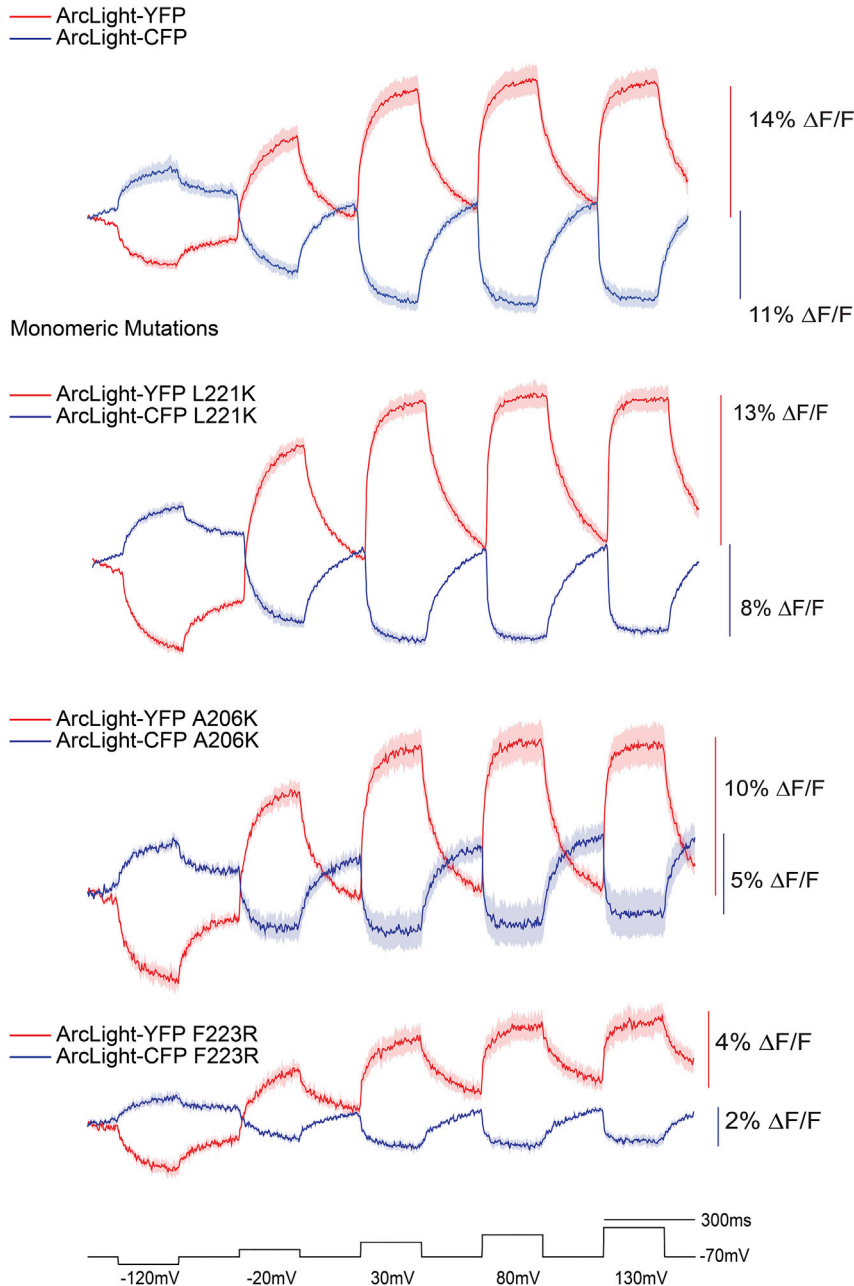
FIGURE 4 Monomeric mutations to the FP domains may reduce but do not destroy the voltage-dependent, intermolecular FRET signal. The top trace is the intermolecular FRET signal reproduced from Fig. 2 C for comparison purposes. The bottom three traces are from HEK cells expressing ArcLight inter- FRET pairs containing one of the three FP monomeric mutations (A206K, L221K, or F223R). The dark trace is the mean from at least four cells. The shaded area is the SE of the mean.

combinations of VSDs with varying voltage sensitivities (Fig. 1). An inter-FRET GEVI pair that responds to very positive membrane potentials will not yield an optical signal during a small depolarization step (Fig. 6 A). The GEVI CC1 is an ArcLight-derived GEVI that has a positively shifted voltage range (12). The $V_{1/2}$ (the membrane potential that corresponds to one half of the total fluorescence change) for CC1 is nearly +100 mV. An inter-FRET GEVI pair that responds to more negative potentials will yield an optical signal for smaller depolarization steps (Fig. 6 B). The $V_{1/2}$ for ArcLight is around −20 mV. By transfecting HEK 293 cells with different combinations of

these VSDs, we could observe the motion of one or both S4 segments, depending on the size of the depolarization step (Fig. 6 C).

When the donor and acceptor FPs are fused to the CC1 voltage-sensing domain, there was no observable signal when the membrane potential was depolarized by 25 mV from a holding potential of −70 mV. In contrast, when the inter-FRET GEVI pair both utilize the voltage-sensing domain from ArcLight, a slow but obvious FRET signal was detected during a 25 mV depolarization (Fig. 6 C). When the membrane potential was depolarized by 100 to +30 mV, both the CC1 FRET pair and the ArcLight
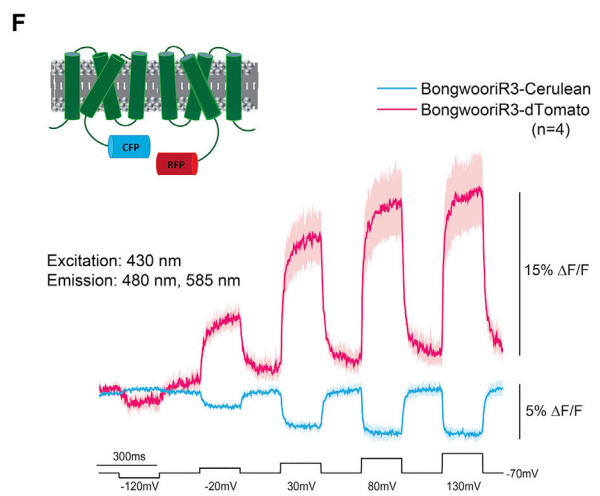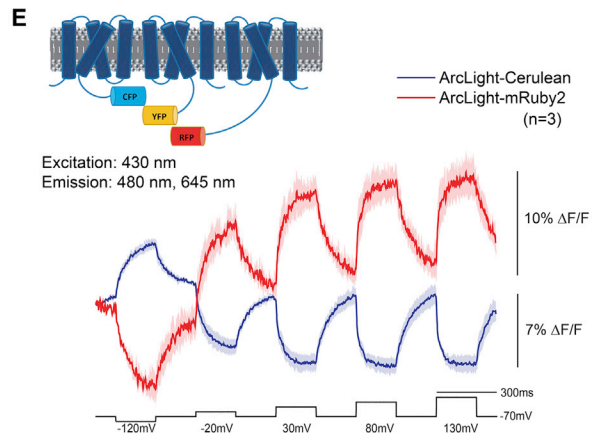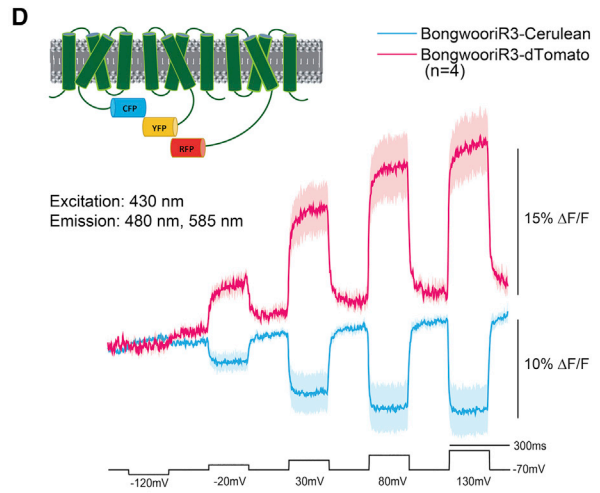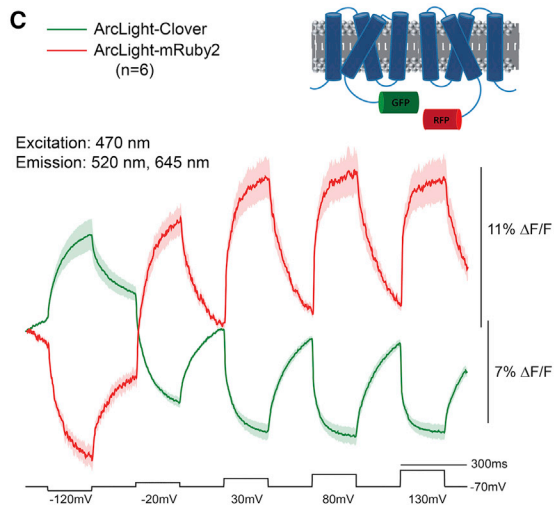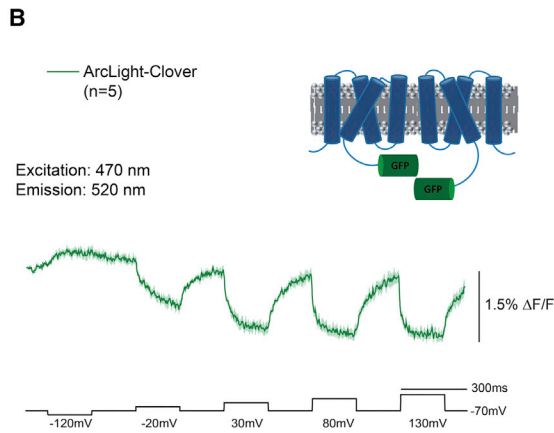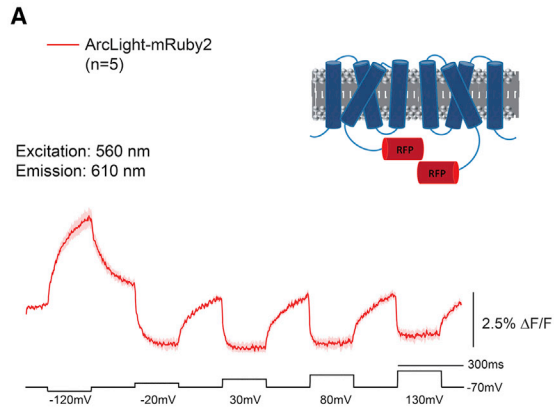
(legend on next page)

FRET pair yielded signals (Fig. 6 C). Because only the voltage-sensing domain from ArcLight responds to the 25 mV voltage step, we then investigated the contribution of donor/donor interactions on the inter-FRET signal by transfecting HEK 293 cells with GEVIs consisting of CC1-CFP and ArcLight-YFP or ArcLight-CFP and CC1-YFP.

When the positively shifted CC1 VSD was fused to the FRET donor and the FRET acceptor was fused to the Arc-Light VSD, a small signal around 1% ΔF/F was observed during the 25 mV depolarization step. This was less than when both FRET FPs were attached to the ArcLight VSD because only one of the two S4 segments was responding. However, when the plasma membrane is depolarized by 100 mV, the signal was nearly twice the size as observed when both FRET pairs were fused to either the CC1 or the ArcLight voltage-sensing domain. This result may be due to the difference in the number of amino acids in the linker segment between the voltage-sensing domain and the FP. For ArcLight, there are 11 amino acids in the linker segment, whereas CC1 has 22 amino acids in the linker segment. The movement of the FP may also be different for the two constructs, which might improve the FRET efficiency for the CC1/ArcLight pairing during stronger depolarization of the plasma membrane. The optical response of CC1/ArcLight FRET pairs during a 50 mV hyperpolarization step and 50, 100, 150, and 200 mV depolarization steps are shown in Fig. S3.

Monitoring the movement of a single FP using lipid anchors

A recurring problem when monitoring inter-FRET GEVI signals is the contamination of the signal caused by homodimers of the FRET donors. Although these signals are small (Figs. 2, A and B and 5), they can still be seen in some recordings. For instance, in Fig. 5 C, when the donor FP is fused to ArcLight and the acceptor FP is fused to the positively shifted CC1 VSDs, the on and off rates for the donor FP do not mirror the rates for the acceptor FP. This is because the donor FP signal is contaminated with the Arc-Light-CFP/ArcLight-CFP voltage-dependent signal as well. This is not the case when the donor FP is fused to positively shifted CC1 construct. There still exists CC1-CFP/CC1-CFP associations, but because CC1 does not respond to that voltage, the FRET signal is less contaminated, resulting in a reduction of the ΔF/F in the CFP channel for the CC1-CFP/ArcLight-YFP pairing. There may still be a contami-

nating signal from ArcLight-YFP/ArcLight-YFP, even though the excitation wavelength was 430 nm.

To remove the contaminating signal from homodimers, we replaced one of the FRET FPs with a farnesylated version lacking a voltage-sensing domain (Fig. 7). When the FRET donor FP CFP is fused to the Bongwoori-R3 VSD and coexpressed in HEK cells with a farnesylated YFP (Fig. 7 A), a 2% ΔF/F for YFP can be seen when the plasma membrane is depolarized by 200 mV. The 200 mV depolarization step results in a 3% ΔF/F signal in the CFP channel. When the FRET pair is reversed by fusing the donor FP to the VSD of Bongwoori-R3, there is still a voltage-dependent FRET signal (Fig. 7 B).

A farnesylated GFP, Clover, was also able to yield a voltage-dependent FRET signal when coexpressed with the GEVI ArcLight-mRuby2 (Fig. 7 C). Again, this signal is much reduced when both FPs are fused to different VSDs, which may indicate that the VSD enhances the association of intermolecular FRET partners. However, we have not tried to optimize the linker link between the FP and the VSD for all of these associations that may also contribute to the dynamic fluorescent signal.

Intermolecular FRET also works for the rhodopsin family of GEVIs (Fig. 7 D). When HEK cells were coexpressed with a farnesylated Clover FP and the rhodopsin GEVI, Ace2N, taken from Ace2N-mNeon (27) lacking the mNeon green domain, a voltage-dependent optical signal was observed. Although this signal is significantly reduced, it provides a proof-of-principle that intermolecular FRET can potentially improve the flexibility for rhodopsin-based GEVIs as well.

DISCUSSION

The experimental paradigm of intermolecular FRET using ArcLight-derived GEVIs has revealed new information about the dimerization mechanism coupling voltage to fluorescence. The suggested homodimer fluorescence mechanism of ArcLight-derived GEVIs that interact via their cytoplasmic FP domains was expanded by the discovery of voltage-dependent intermolecular FRET signals (Figs. 2 and 3). The observation that monomeric mutations to the FP dramatically reduced the voltage-dependent optical signal of ArcLight suggested that the association was primarily via the FP domain (11). However, the intermolecular FRET signals have revealed that the interaction between the FPs of adjacent GEVIs persists despite the presence of monomeric mutations to the FP domain (Fig. 4), suggesting

FIGURE 5 Expanding the spectrum of inter-FRET GEVIs. (A) ArcLight-mRuby2. The trace is the average of five HEK cells expressing ArcLight-mRuby2. (B) ArcLight-Clover. The trace is the average from five HEK cells expressing ArcLight-Clover. (C) Coexpression of ArcLight-Clover/Arc-Light-mRuby2. The traces are from six HEK cells. (D) Triple transfection with BongwooriR3-Cerulean/BongwooriR3-Venus/BongwooriR3-dTomato. Traces are the average of four cells. (E) Triple transfection with ArcLight-Cerulean/ArcLight-Venus/ArcLight-mRuby2. The traces are the averages of three cells. (F) Coexpression of BongwooriR3-Cerulean/BongwooriR3-dTomato. The traces are the averages of four cells. The voltage steps are in black. In all cases, the dark trace is the mean, and the shaded area is the standard deviation of the mean.
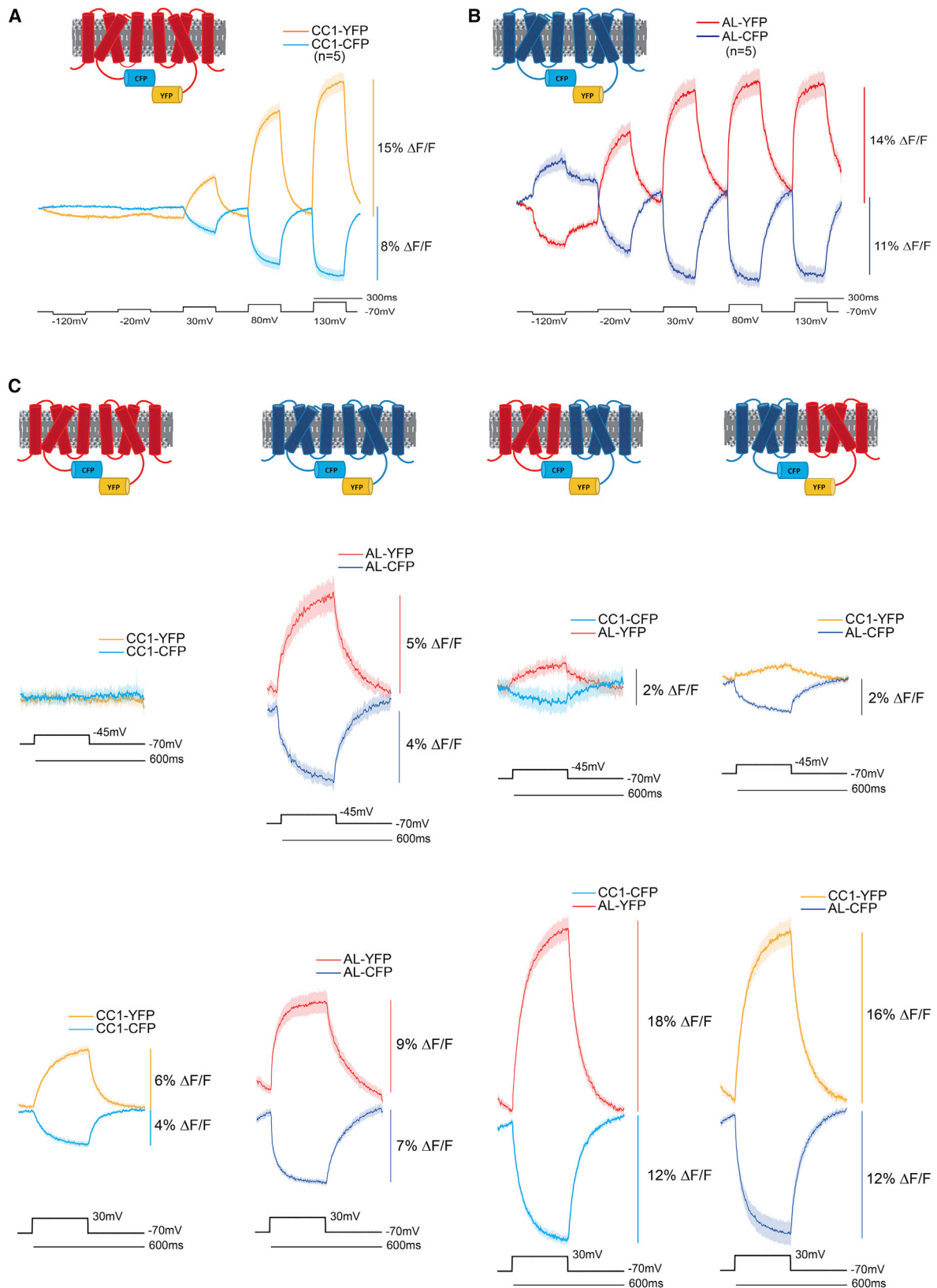
FIGURE 6 Decoupling the voltage-dependent FRET signal by varying the voltage sensitivities of the voltage-sensing domains. (*A*) An inter-FRET GEVI pair using the voltage-sensing domain from CC1 (*red transmembrane segments*) that has a positively shifted voltage responsive range. The donor fluorescence trace is in light blue (CC1-CFP). The acceptor fluorescence trace is in yellow (CC1-YFP). Voltage steps are in black. (*B*) An intermolecular FRET GEVI

(legend continued on next page)

other regions of potential interactions. A recent study reported that the intact voltage-sensing *C. intestinalis* phosphatase Ci-VSP can dimerize (22). Because the voltage-sensing phosphatase lacks an FP domain and the intermolecular FRET GEVIs lack the phosphatase domain, the voltage-sensitive domain is likely responsible, at least in part, for dimerization.

The association of the voltage-sensitive domain enabled the development of a new family of inter-FRET GEVIs by fusing the donor FP to one VSD and the acceptor FP onto a separate VSD. We can now create GEVIs that can do the following: 1) get brighter in response to depolarization, 2) have inverted signals that can be used to remove motion artifacts, 3) improve the dynamic range by amplifying the voltage-induced conformational change, 4) exploit multiple wavelengths, 5) permit the development of better two-photon voltage sensors, and 6) restrict expression to more precisely defined cellular populations.

ArcLight has a large dynamic response to membrane potential changes and gets dimmer upon depolarization of the plasma membrane (10). In an independent comparison of GEVIs from 2019, ArcLight was the only GEVI capable of reporting neuronal activity in response to visual stimuli in the mouse visual cortex (8). Unfortunately, the signal/noise ratio is low for several reasons. One is that the optically responsive protein is limited to the plasma membrane, which generates a high background fluorescence because dendrites as well as axons are fluorescent (28). Another is that the voltage change experienced by a neuron can vary from small depolarizing or hyperpolarizing synaptic potentials that last tens of milliseconds to large voltage changes from action potentials that last 1–2 ms. One way to reduce the high background is to create a GEVI that starts dim and gets brighter upon depolarization. Several rhodopsin-based GEVIs exhibit this characteristic but require intense illumination, which limits the number of cells that can be imaged simultaneously (1,29). The rhodopsin-based GEVIs also respond poorly upon two-photon illumination and exhibit light-induced currents as well as chromogenic effects. Two ArcLight-derived GEVIs have been developed that also become brighter upon depolarization of the plasma membrane, FlicR1 which has the added advantage of being red-shifted (30) and Marina (31). Both show promise but have not yet exhibited the large change in fluorescence that ArcLight has.

Intermolecular FRET GEVIs offer an alternative solution to this problem. Depending on the emission wavelength being monitored, the voltage-induced optical signal can start bright and get dimmer during depolarization, or it start dim and get brighter (Figs. 2, 3, and 5). With the use of an optical splitter, both emission wavelengths can be monitored simultaneously, enabling the removal of motion artifacts. Motion artifacts will affect the fluorescence in both emission wavelengths similarly, whereas a voltage-induced change would generate opposite fluorescent signals in the two emission channels. In addition, the inter-FRET GEVIs can utilize any FRET pair, CFP/YFP (Figs. 2, 3, and 4), GFP/RFP (Fig. 5 *C*), and CFP/RFP (Fig. 5, *D–F*). In the case of the CFP/RFP pairing, the signal was separated from the excitation wavelength by over 200 nm, which we believe is a record for GEVIs. Although this may not be an ideal pairing (the transfer efficiency may be too low), having the emission wavelength get brighter upon depolarization and be 200 nm away from the excitation wavelength could be an ideal situation for some in vivo recordings. In the future, we plan to expand the repertoire of FPs to include those that are very bright under two-photon illumination for use as the inter-FRET GEVI donor in combination with an appropriate FP acceptor.

Another advantage of inter-FRET GEVIs is that the dynamic range is improved because the conformational change is the result of the movement of two VSDs (Fig. 6). Having the donor and acceptor FPs on separate proteins enables the mixing of heterogeneous voltage-sensitive domains. By combining a voltage-sensing domain that only responds to very positive potentials (Fig. 6 *A*) with a voltage-sensing domain that responds to physiologically relevant voltages (Fig. 6 *C*), an experimenter can control the movement of one or both by clamping the plasma membrane to different potentials. To verify that the movement of only the FRET donor or only the FRET acceptor could elicit a voltage-dependent optical signal, coexpression of inter-FRET GEVIs with a farnesylated partner lacking a voltage-sensing domain were also able to respond to potential changes (Fig. 7). The signal size of inter-FRET GEVIs partnered with a farnesylated FP were reduced roughly five-fold, suggesting that two VSDs improves the association of the GEVIs and/or that the linker length for the farnesylated FP pairing is not optimal. Despite the reduced optical signal, the fact that a voltage-dependent FRET signal can occur between two membrane proteins creates the possibility that any membrane protein could be used as a potential FRET partner. The voltage-dependent FRET signal could then be limited to different parts of the cell, such as the axon or

using the voltage-sensing domain from ArcLight (*blue transmembrane segments*) that responds to more negative membrane potentials. The donor fluorescence trace is in dark blue (AL-CFP). The acceptor fluorescence trace is in red (AL-YFP). (*C*) Four columns of the different combinations of CC1 and ArcLight inter-FRET GEVI pairs. The top row of traces are from HEK cells experiencing a 25 mV depolarization of the plasma membrane potential. The bottom row of traces are from HEK cells experiencing a 100 mV depolarization of the plasma membrane potential. The colors of the traces and voltage-sensing domains are as described in (*A*) and (*B*). Excitation wavelength was 430 nm for all experiments. CFP emission was measured at 480 nm, and YFP emission was measured at 540 nm. All traces are the averages from six cells. The solid line in the traces represents the mean and the shaded area is the standard error of the mean.

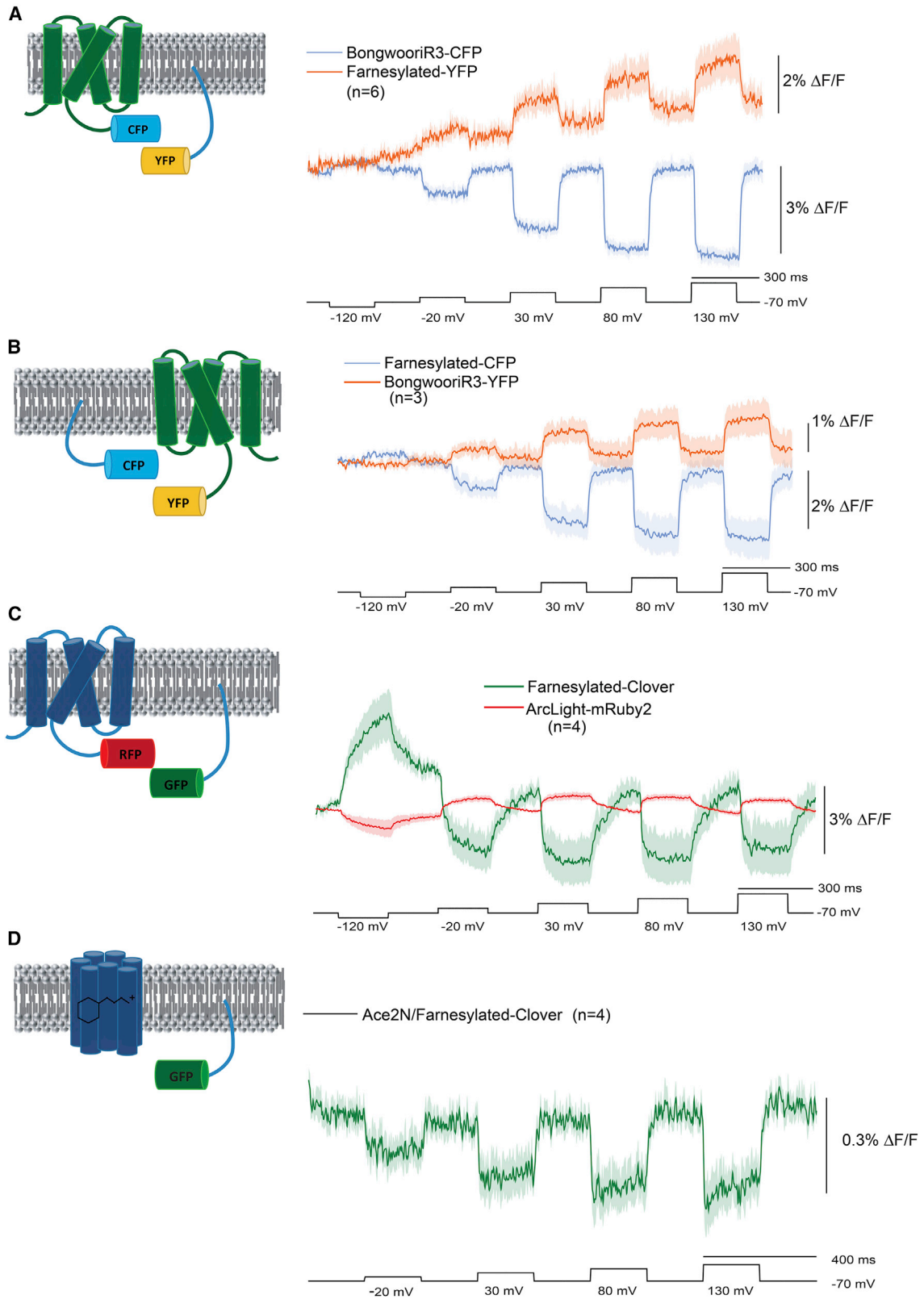FIGURE 7 Intermolecular FRET with a farnesylated FP. (A) CFP fused to the voltage-sensing domain of the GEVI Bongwoori-R3 was coexpressed in HEK cells with a farnesylated version of YFP. The blue trace is the emission at 480 nm. The red trace is the emission at 540 nm. The excitation wavelength

(legend continued on next page)

synapse. This may also be true for the electrochromic FRET GEVIs that utilize bacterial rhodopsin, such as Ace2N-mNeon (27).

Inter-FRET GEVIs also have the potential advantage of finely refining the neuronal cell type expressing both the donor and acceptor FRET GEVIs via intersectional targeting (32). By placing the expression of the FRET donor GEVI under one promoter and the expression of the FRET acceptor GEVI under another promoter, only cells capable of expressing both would yield a voltage-dependent FRET signal. Although this could enhance the decoding of neuronal circuits, a hurdle preventing the current use of inter-FRET GEVIs in vivo is the need to proportionally express both GEVIs at levels facilitating heterodimer formation. In culture, this is relatively easy because both constructs are expressed at high levels. Indeed, we did not need to optimize transfection levels to observe inter-FRET GEVI signals. However, in vivo, this is not a trivial issue. This problem with variable expression is compounded with the formation of homodimers. Once the dimer site is identified, homodimers can be disrupted. Further modifications of the dimer may facilitate only heterodimer formation. Once these challenges are met, the advantages of inter-FRET GEVIs should be realized.

SUPPORTING MATERIAL

Supporting material can be found online at https://doi.org/10.1016/j.bpj.2021.03.010.

AUTHOR CONTRIBUTIONS

L.M.L. designed experiments, performed experiments, analyzed data, and assisted in writing the text. B.E.K. performed experiments and analyzed data. B.J.B. designed experiments, analyzed data, and assisted in writing the text.

ACKNOWLEDGMENTS

REFERENCES

1. Adam, Y., J. J. Kim, …, A. E. Cohen. 2019. Voltage imaging and optogenetics reveal behaviour-dependent changes in hippocampal dynamics. *Nature.* 569:413–417.

2. Kannan, M., G. Vasan, …, V. A. Pieribone. 2018. Fast, in vivo voltage imaging using a red fluorescent indicator. *Nat. Methods.* 15:1108–1116.

3. Marshall, J. D., J. Z. Li, …, M. J. Schnitzer. 2016. Cell-type-specific optical recording of membrane voltage dynamics in freely moving mice. *Cell.* 167:1650–1662.e15.

4. Piatkevich, K. D., E. E. Jung, …, E. S. Boyden. 2018. A robotic multidimensional directed evolution approach applied to fluorescent voltage reporters. *Nat. Chem. Biol.* 14:352–360.

5. Yi, B., B. E. Kang, …, B. J. Baker. 2018. A dimeric fluorescent protein yields a bright, red-shifted GEVI capable of population signals in brain slice. *Sci. Rep.* 8:15199.

6. Lee, S., T. Geiller, …, B. J. Baker. 2017. Improving a genetically encoded voltage indicator by modifying the cytoplasmic charge composition. *Sci. Rep.* 7:8286.

7. Chamberland, S., H. H. Yang, …, F. St-Pierre. 2017. Fast two-photon imaging of subcellular voltage dynamics in neuronal tissue with genetically encoded indicators. *eLife.* 6:e25690.

8. Bando, Y., M. Sakamoto, …, R. Yuste. 2019. Comparative evaluation of genetically encoded voltage indicators. *Cell Rep.* 26:802–813.e4.

9. Ng, M., R. D. Roorda, …, G. Miesenböck. 2002. Transmission of olfactory information between three populations of neurons in the antennal lobe of the fly. *Neuron.* 36:463–474.

10. Jin, L., Z. Han, …, V. A. Pieribone. 2012. Single action potentials and subthreshold electrical events imaged in neurons with a fluorescent protein voltage probe. *Neuron.* 75:779–785.

11. Kang, B. E., and B. J. Baker. 2016. Pado, a fluorescent protein with proton channel activity can optically monitor membrane potential, intracellular pH, and map gap junctions. *Sci. Rep.* 6:23865.

12. Piao, H. H., D. Rajakumar, …, B. J. Baker. 2015. Combinatorial mutagenesis of the voltage-sensing domain enables the optical resolution of action potentials firing at 60 Hz by a genetically encoded fluorescent sensor of membrane potential. *J. Neurosci.* 35:372–385.

13. Sung, U., M. Sepehri-Rad, …, B. J. Baker. 2015. Developing fast fluorescent protein voltage sensors by optimizing FRET interactions. *PLoS One.* 10:e0141585.

14. Dimitrov, D., Y. He, …, T. Knöpfel. 2007. Engineering and characterization of an enhanced fluorescent protein voltage sensor. *PLoS One.* 2:e440.

15. Lundby, A., W. Akemann, and T. Knöpfel. 2010. Biophysical characterization of the fluorescent protein voltage probe VSFP2.3 based on the voltage-sensing domain of Ci-VSP. *Eur. Biophys. J.* 39:1625–1635.

16. Akemann, W., H. Mutoh, …, T. Knöpfel. 2012. Imaging neural circuit dynamics with a voltage-sensitive fluorescent protein. *J. Neurophysiol.* 108:2323–2337.

17. Rizzo, M. A., G. H. Springer, …, D. W. Piston. 2004. An improved cyan fluorescent protein variant useful for FRET. *Nat. Biotechnol.* 22:445–449.

18. Nagai, T., K. Ibata, …, A. Miyawaki. 2002. A variant of yellow fluorescent protein with fast and efficient maturation for cell-biological applications. *Nat. Biotechnol.* 20:87–90.

19. von Stetten, D., M. Noirclerc-Savoye, …, A. Royant. 2012. Structure of a fluorescent protein from Aequorea victoria bearing the obligate-monomer mutation A206K. *Acta Crystallogr. Sect. F Struct. Biol. Cryst. Commun.* 68:878–882.

20. Espagne, A., M. Erard, …, F. Mérola. 2011. Cyan fluorescent protein carries a constitutive mutation that prevents its dimerization. *Biochemistry.* 50:437–439.

was 430 nm. Dark line is the mean of six cells. Shaded areas are the SE of the mean. (*B*) YFP fused to the voltage-sensing domain of Bongwoori-R3 was coexpressed with a farnesylated CFP. The color coding and wavelengths are as in (*A*). (*C*) The FP mRuby2 was fused to the GEVI ArcLight and coexpressed with a farnesylated Clover FP. The green trace is the emission at 520 nm. The red trace is the emission at 585 nm. The excitation wavelength is 470 nm. (*D*) Intermolecular FRET of a rhodopsin GEVI, Ace_2N (27), lacking the mNeon FP was coexpressed with farnesylated-Clover.

21. Zacharias, D. A., J. D. Violin, …, R. Y. Tsien. 2002. Partitioning of lipid-modified monomeric GFPs into membrane microdomains of live cells. *Science.* 296:913–916.

22. Rayaprolu, V., P. Royal, …, S. C. Kohout. 2018. Dimerization of the voltage-sensing phosphatase controls its voltage-sensing and catalytic activity. *J. Gen. Physiol.* 150:683–696.

23. Lam, A. J., F. St-Pierre, …, M. Z. Lin. 2012. Improving FRET dynamic range with bright green and red fluorescent proteins. *Nat. Methods.* 9:1005–1012.

24. Villalba-Galea, C. A., W. Sandtner, …, F. Bezanilla. 2009. Charge movement of a voltage-sensitive fluorescent protein. *Biophys. J.* 96:L19–L21.

25. Treger, J. S., M. F. Priest, and F. Bezanilla. 2015. Single-molecule fluorimetry and gating currents inspire an improved optical voltage indicator. *eLife.* 4:e10482.

26. Perron, A., H. Mutoh, …, T. Knöpfel. 2009. Second and third generation voltage-sensitive fluorescent proteins for monitoring membrane potential. *Front. Mol. Neurosci.* 2:5.

27. Gong, Y., C. Huang, …, M. J. Schnitzer. 2015. High-speed recording of neural spikes in awake mice and flies with a fluorescent voltage sensor. *Science.* 350:1361–1366.

28. Nakajima, R., and B. J. Baker. 2018. Mapping of excitatory and inhibitory postsynaptic potentials of neuronal populations in hippocampal slices using the GEVI, ArcLight. *J. Phys. D Appl. Phys.* 51:504003.

29. Lou, S., Y. Adam, …, A. E. Cohen. 2016. Genetically targeted all-optical electrophysiology with a transgenic Cre-dependent optopatch mouse. *J. Neurosci.* 36:11059–11073.

30. Abdelfattah, A. S., S. L. Farhi, …, R. E. Campbell. 2016. A bright and fast red fluorescent protein voltage indicator that reports neuronal activity in organotypic brain slices. *J. Neurosci.* 36:2458–2472.

31. Platisa, J., G. Vasan, …, V. A. Pieribone. 2017. Directed evolution of key residues in fluorescent protein inverses the polarity of voltage sensitivity in the genetically encoded indicator ArcLight. *ACS Chem. Neurosci.* 8:513–523.

32. Madisen, L., A. R. Garner, …, H. Zeng. 2015. Transgenic mice for intersectional targeting of neural sensors and effectors with high specificity and performance. *Neuron.* 85:942–958.